QUICKBIRD 2 TASSELED CAP TRANSFORM COEFFICIENTS: A COMPARISON OF DERIVATION METHODS

Lance D. Yarbrough
Department of Geology and Geological Engineering,
University of Mississippi, 118 Carrier Hall,
University, Mississippi 38677
www.geo.olemiss.edu
The University of Mississippi Geoinformatics Center,
University, Mississippi 38677
www.umgc.olemiss.edu
lance@yarbrough.com

Greg Easson
Department of Geology and Geological Engineering,
University of Mississippi, 118 Carrier Hall,
University, Mississippi 38677
The University of Mississippi Geoinformatics Center,
University, Mississippi 38677
www.umgc.olemiss.edu
Enterprise for Innovative Geospatial Solutions,
University, Mississippi 38677
www.eigs.olemiss.edu
geasson@olemiss.edu

Joel S. Kuszmaul
Department of Geology and Geological Engineering,
University of Mississippi, 118 Carrier Hall,
University, Mississippi 38677
kuszmaul@olemiss.edu

ABSTRACT

As remote sensing sensors and data systems become more complex, the need for a simple, meaningful index becomes essential in applications. It is also a key component to any successful data product distribution to create equivalent outputs when compared to past sensor capabilities. This continuity of data and traditional indices will become more important with the approaching Landsat *gap* and after the next-generation of the earth observation sensors are placed in orbit.

The Tasseled Cap Transform (TCT) is a practical vegetative index and spectral enhancement and has been adapted to other multispectral sensors; most notability, the TM, ETM+ and ASTER. Unfortunately, there have been modifications to the Tasseled Cap derivation presented in literature that have created confusion regarding the transform and the proper orientation of the defined feature space.

The TCT coefficients for DigitalGlobe's QuickBird 2 (QB) sensor were derived using three different techniques, each based on the original description of the Tasseled Cap defined feature space. All three techniques achieved nearly the same results. The method based on the Gram-Schmidt Orthogonalization method was the most useful with the QB sensor. This derivation technique was used to create the final reported set of Tasseled Cap coefficients for the 11-bit, DRA-off QB product.

INTRODUCTION

Kauth and Thomas (1976) define the special feature space known as *Tasseled Cap space*. This special feature space is defined by coordinate axes that are characteristic of the physical features within the imagery. The Tasseled Cap Transform (TCT) projects spectral space coordinates (i.e. DN_{band1}, DN_{band2}) onto Tasseled Cap space (i.e.

$u_{Brightness}$, $u_{Greenness}$, $u_{Wetness}$). A benefit of the TCT is its ability to compress data. The variance represented by highly correlated spectral space coordinates can be captured with few dimensions in Tasseled Cap space. The goal of the research was to compare three well-cited methods of deriving Tasseled Cap Transform coefficients.

The Nature of Tasseled Cap Space

Tasseled Cap space takes advantage of the correlated spectral space, typical of optical multispectal sensors recording data with visual/near-infrared and shortwave regions of the electromagnetic spectrum. Distinct directions exist which represent characteristic features within the scene. Figure 1 illustrates these characteristic directions by plotting the data in spectral space coordinates (11-bit DN).

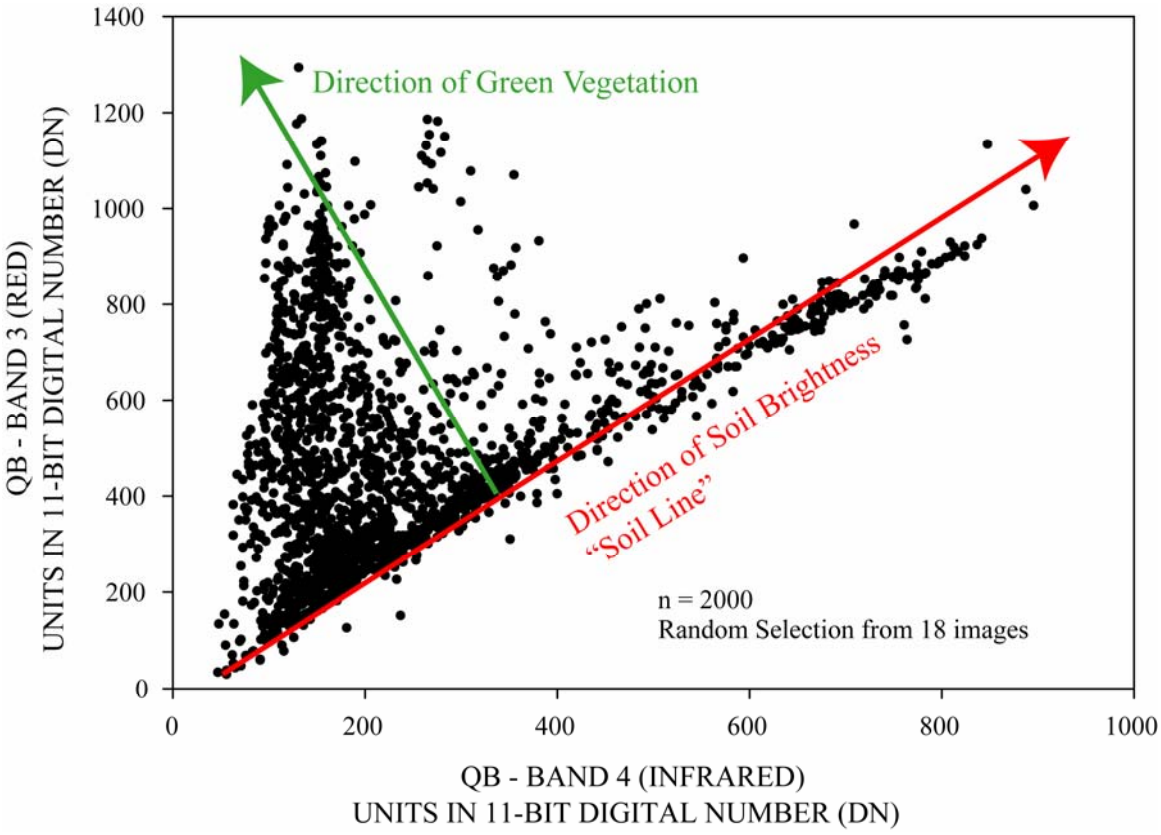

Figure 1. QuickBird 2 Band 4 versus Band 3.

METHODS

Kauth and Thomas (1976) refer to the transform space as the fixed feature space, which has its coordinate axes aligned in the Tasseled Cap directions (e.g. Brightness, Greenness, Wetness). To accomplish this alignment, the linear transform is defined as:

$$\mathbf{u} = \mathbf{W}_{TC}\mathbf{x} + \mathbf{r} \quad (1)$$

where **x** is the DN value of the QB 11-bit data, $\mathbf{W}_{TC}$ is the unitary (or orthogonal) transform matrix, and the vector **r** is an offset vector that was used to both maintain positive coordinate values of TCT vector **u** and to compare TCTs from one sensor to another (Kauth and Crist, 1986). The literature presents two general categories of TCT coefficient derivation whereby the vectors within $\mathbf{W}_{TC}$ are discovered.

The first category is methods that use the Gram-Schmidt Orthogonalization process. The second general category is more loosely defined as those methods that use statistical approaches such as covariance or correlation matrices as basis for deriving the TCT coefficients. The analysis most supported in literature is the Principle Component Transform (Crist and Cicone, 1984; Crist and Kauth, 1986; Huang et al., 2002, Horne, 2003; Yarbrough et al., 2005).

The Gram-Schmidt Orthogonalization process was first used by Kauth and Thomas (1976) used to create the TCT coefficients. Ideally, it should be used with a three- or four-band sensor. It begins the defined feature space with the $\mathbf{u}_{Brightness}$ or soil brightness coordinate axis. This is a benefit in that it removes bias when defining the soil brightness direction. This iterative process continues with defining the Greenness and Wetness axes on a orthogonal basis.

Principle Component Transform (PCT) was used when the sensor began to contain more than four bands (Crist and Cicone, 1984). Compared to the Gram-Schmidt, the PCT is less laborious but only offers initial eigenvectors for the new transform. To create the defined feature Tasseled Cap space, additional rotations within the initial eigenspace are required. These rotations are subjective and based on the perceived shape of data within the transformed space.

Location	Date
Wenona, Illinois	16-Sep-03
	12-Apr-03
Blue Earth, Minnesota	26-Jul-03
	06-Oct-03
Enid, Oklahoma	05-Aug-03
	08-Apr-04
Casa Grande, Arizona	15-Apr-03
	14-Jul-03
Grandview, Washington	23-Aug-03
	21-Oct-03
Szczecin, Poland	18-Mar-03
	22-Sep-03
Goiania, Brazil	23-Apr-03
	11-Aug-04
Cambridge, England	16-Oct-03
	29-Mar-02
London, Ohio	01-Sep-02
	21-Oct-03
Austin, Texas	17-Dec-03
	23-Jul-03

Table 1. Location and dates of imagery.

Image Selection

Researchers in the initial investigations of TCT derivations used imagery from the Midwest agricultural regions of the United States. Typically the number of scenes used and the time period were limited. As methods progressed and computing systems began to accommodate larger datasets, the number of scenes used in an analysis increased. Horne (2003) used all the pixel values of 195 scenes of IKONOS imagery, while Kauth and Thomas (1979), simply acquired selected pixel values from a subset of a single MSS scene.

With the increase of scenes came the ability for an investigator to account for higher variance during the growing season. Soil moisture, senescence, other phenomena and there effect on the reflectance of a specific feature could be introduced into the variance calculations. The images used in the study were selected based on the following criteria:

Two scenes which spatially overlay or nearly overlay and
Both represent differing times within the growing season(s)
Scenes which are nearly cloud-free
Scenes representing >88% forested and agricultural features
Scenes containing some water features yet represents less than 2% of all pixels within the image

Eighteen of the twenty images listed in Table 1 meet all above criteria. The dates for each of the acquisitions are listed. Casa Grande, Arizona scenes were excluded from the final coefficient derivations. During the archive search of DigitalGlobe's image database, the five listed criteria were found to be extremely limiting. Therefore, four scenes (two locations) chosen contain a larger percentage of invariant feature and urban signatures than initially allowed. The criteria were relaxed to allow as much as 12% of the scene to contain non-vegetative features.

Effects of desert agriculture

Two scenes highlighted in Table 1, are located near Casa Grande, Arizona. This is an agricultural area in the Soñoran Desert of Southern Arizona, approximately 70 kilometers northwest of Tucson, Arizona. The common crops grown in the area are cotton, alfalfa, and pecans. Both images contain well-contrasted agricultural fields, irrigation ditches and canals within a desert landscape. These scenes were used to compare intermediate steps of the three different derivation methods. They also provided a way to assess qualitatively the sensitivity of the derivation methods.

Gram-Schmidt Orthogonalization Process

Kauth and Thomas (1976) first used the Gram-Schmidt Orthogonalization process to derive TCT coefficients. This method is a sequential process to determine the orthogonal basis for a given set of vectors. In the case of the TCT, the soil line is determined and the vector in the "brightness" direction. From that basis vector, all other vectors are orthogonally constructed. Generally, these orthogonal set of vectors are normalized resulting in a final set of orthonormal basis vectors.

The Gram-Schmidt process or construction is found in any introductory linear algebra textbook. However, to insure this process is understood with respect to Tasseled Cap space, we will elaborate more on the specific steps of the Gram-Schmidt Orthogonalization process. The general process follows as:

Select first vector as the initial basis vector direction
Select second vector of desired direction and orthogonally project onto the first basis vector
Select third vector and orthogonally project onto the first and second basis vectors
Select fourth vector direction and orthogonally project onto the first three basis vectors

This process is expressed as:

$$\mathbf{u}_i = \mathbf{v}_i - \sum_{n=1}^{i-1} \frac{\langle \mathbf{v}_i, \mathbf{u}_n \rangle}{\langle \mathbf{u}_n, \mathbf{u}_n \rangle} \mathbf{u}_n \tag{2}$$

where $\mathbf{u}_i$ is the linear combination of the selected vector direction and previous basis vectors. Again, this process produces a set of orthogonal basis vectors. Customarily, at the completion of Gram-Schmidt process, all basis vectors are normalized by dividing each vector by its own length:

$$\hat{\mathbf{u}}_i = \frac{1}{\|\mathbf{u}_i\|} \mathbf{u}_i \tag{3}$$

To limit confusion, this paper reports all basis vectors as orthonormal basis vectors, meaning that they are mutually perpendicular or the inner product $\langle \mathbf{u}_i, \mathbf{u}_j \rangle = 0$ when $i \neq j$ and they each have a unit length of 1 or $\langle \mathbf{u}_i, \mathbf{u}_i \rangle = 1$.

Using the Gram-Schmidt Orthogonalization method, the vector in the direction of the soil line was selected as the basis vector for the brightness coordinate axis. First the soil line, $\mathbf{v}_1$ became the new coordinate axis, $\mathbf{u}_{Brightness}$. Next, the vector in the direction of the healthy agricultural vegetation was selected as $\mathbf{v}_2$. Continuing the Gram-Schmidt Orthogonalization process, vector $\mathbf{v}_2$ was orthogonally projected onto the subspace defined by the direction of the Tasseled Cap axes. This new basis vector, $\mathbf{u}_{Greenness}$ was defined by the following relationship:

$$\mathbf{u}_{Greenness} = \mathbf{v}_2 - \frac{\langle \mathbf{v}_2, \mathbf{u}_{Brightness} \rangle}{\langle \mathbf{u}_{Brightness}, \mathbf{u}_{Brightness} \rangle} \mathbf{u}_{Brightness} \tag{4}$$

where the projection of the $\mathbf{v}_2$ onto the normalized unit vector of the first coordinate axis.

Using Gram-Schmidt Orthogonalization process yielded two orthogonal vectors: one in the direction of the soil brightness and the other in the direction of healthy agricultural vegetation. We continued the process until all four vectors representing the appropriate direction of concern were orthogonal with respect to each other. Again, all basis vectors were normalized prior to reporting as $\mathbf{W}_{TC}$.

Propagation of Error

The Gram-Schmidt process builds on the previous approximation of other vector projection. Because of this iterative nature, rounding errors when calculating the inner products of vectors will occur. This error will continue to propagate through the construction process with the last vector projected containing the most possible error. The nature of the Tasseled Cap space tends to minimize this error effect in lower order TCT coordinate axes. The soil brightness and vegetation are commonly selected as the first two TCT coordinate axes directions. These two directions typically account for 95-99% of all variance and contain the least error of the Gram-Schmidt process. Higher order axes in Tasseled Cap space will contain greater effects of noise and greater effects of error due to the approximation process.

Other Orthogonalization Methods

Methods similar to the Gram-Schmidt exist in the field of linear algebra. One such process is the "double-step" version of the Gram-Schmidt process. This process acknowledges the issue of rounding errors in the "single-step" Gram-Schmidt process and reduces the error by transposing the first result of the Gram-Schmidt. An additional orthogonalization process is undertaken and that result is again transposed to reestablish the row or column vector orientation of the original matrix.

Because of the nature of the TCT and the fact that all reported vectors are orthonormal, the representative transform coefficients only require an accuracy of 10^{-6} and are found in the literature reported to an accuracy of 10^{-3}. The rounding error typically found in the "single-step" Gram-Schmidt process involving four vectors is approximately 10^{-16}, while the reduced error in the "double-step" process is commonly 10^{-21} (Foxes, 2005). Given the reporting accuracy, the propagation of the rounding error will not become significant until 20 or more vectors are used in the process. Even so, the effects of additional spectral bands tend to bias the Tasseled Cap space when linear combinations are calculated. The greatest numbers of spectral bands used in a TCT derivation were the nine-reflectance bands of the Terra ASTER sensor (Yarbrough et al., 2005).

Principle component initialization

As previously mentioned the principle component method (PCT) is the most cited derivation technique in the literature. The PCT allows the investigator to identify the eigenspace that explains the variance of the dataset. The eigenvalues and associated eigenvectors become a starting point from which an investigator rotates the feature space into the feature space defined by the Tasseled Cap coordinate axes.

One of the benefits of the PCT method is the speed at which a set of pixels can be projected onto Principle Component space. If using whole images, the initial eigenvectors are obtained with little effort on the part of the investigator. Unfortunately, these initial eigenvectors commonly yield linear combinations that bare little resemblance to Tasseled Cap space. Again, due to the nature of Tasseled Cap space, it is serendipitous that the coordinate axes align with Principle Component space. The resulting feature space must be properly rotated onto the properly define feature space. This task involves plotting data and estimating the required rotation angles. Depending on the number of spectral bands and the complexity of the feature space, this can prove challenging. It is usually most productive to view the data within each 2-D plane of the coordinate system. Guidelines are usually plotted to assist the investigator in the rotations (Figure 2).

This process is well documented in the literature and has been shown to be more useful in sensors containing four or more spectral bands. Compared to the Gram-Schmidt process, after the data are vetted, there are fewer preliminary steps required for this derivation technique. The majority of the work involved is performed after the initial eigenvectors are calculated.

Methods of selecting data

The literature supports two methods of selecting data for the PCT derivation technique. Prior to hardware and software applications advancements, investigators selected random pixels (approx. 2000) from the candidate images. These selected pixels are used in the PCT technique. From there, whole image ingestion and use of all valid pixels have been used. For the 18 QB scenes used in the whole image ingestion in our research, approximately 630 million pixels were used to calculate the variance-covariance matrix of the data.

For the QB imagery used in Table 1, the results of the randomly selected pixels compared to whole image ingestion method were nearly identical. The following are the eigenvalues reported from the PCT:

$$\Lambda_{random2k} = [83737.3 \quad 28611.9 \quad 702.2 \quad 234.9] \tag{5}$$

$$\Lambda_{wholeimage} = [85891.8 \quad 26882.3 \quad 737.1 \quad 71.0] \tag{6}$$

The relative magnitudes of these eienvalues are nearly the same. Because of this similarity, we did not continue the rotations of the 2000 randomly selected pixels. These eigenvalues represent the axis of the hyperellipsoid containing the data space. The goal of performing the PCT was to obtain initial eigenvectors. Because these eigenvectors were rotated into a separately defined feature space, yet with identical coordinate axes directions, there is little need to duplicate this process based on the nearly identical eigenvaules.

RESULTS AND DISCUSSION

The results from the three different methods were nearly identical when comparing the plots of Tasseled Cap coordinates (Figure 2). The first three coordinate axes, Brightness, Greenness and Wetness, tended to align well with the characteristic directions of the data space. A visual inspection of the data space involving the fourth coordinate axis was not preformed. Therefore, no name is given to the fourth TCT axis. Using the row vector in Equation 5 as an example, the variance represented by the relative length, λ_4 of the fourth coordinate axis was approximately 0.21% and the data contained a high degree of noise as evident in Figure 3(D).

The following are the TCT coefficients for QB DN 11-bit data derived using the Gram-Schmidt Orthogonalization Process:

$$\mathbf{W}_{TCT} = \begin{pmatrix} 0.319 & -0.121 & 0.652 & 0.677 \\ 0.542 & -0.331 & 0.375 & -0.675 \\ 0.490 & -0.517 & -0.639 & 0.292 \\ 0.604 & 0.780 & -0.163 & 0.011 \end{pmatrix} \tag{7}$$

where the matrix is the column eigenvectors representing the coefficients for each spectral band. The subsequent linear combination yielded the Tasseled Cap space coordinate of Equation 1. To calculate the Brightness coordinate of a pixel projected onto Tasseled Cap space, the linear combination follows as:

$$u_{Brightness} = 0.319x_{blue} + 0.542x_{green} + 0.490x_{red} + 0.604x_{nir}\,. \tag{8}$$

The remaining Tasseled Cap coordinates were calculated using the appropriate coefficients for each linear combination. We offer the ERDAS .gmd model file and TAB delimited row vector file of Equation 7 on our web site. The delimited file is easily imported into ENVI, PCI or MATLAB software.

For the easy visualization, imagine the eigenvalues as the length of axes for an ellipse within n-dimensional space. Since the QB data is four dimensional in nature, these four eigenvalues can be considered the lengths of the axes for a hyperellipsoid in 4-D space. Because the first two eigenvectors are far greater in magnitude than the others, the above eigenvalues in Equations 5 and 6 are analogous to a 2-D ellipse within 4-D space. Nearly all the variance within the system can be explained when using only the first two eigenvalues.

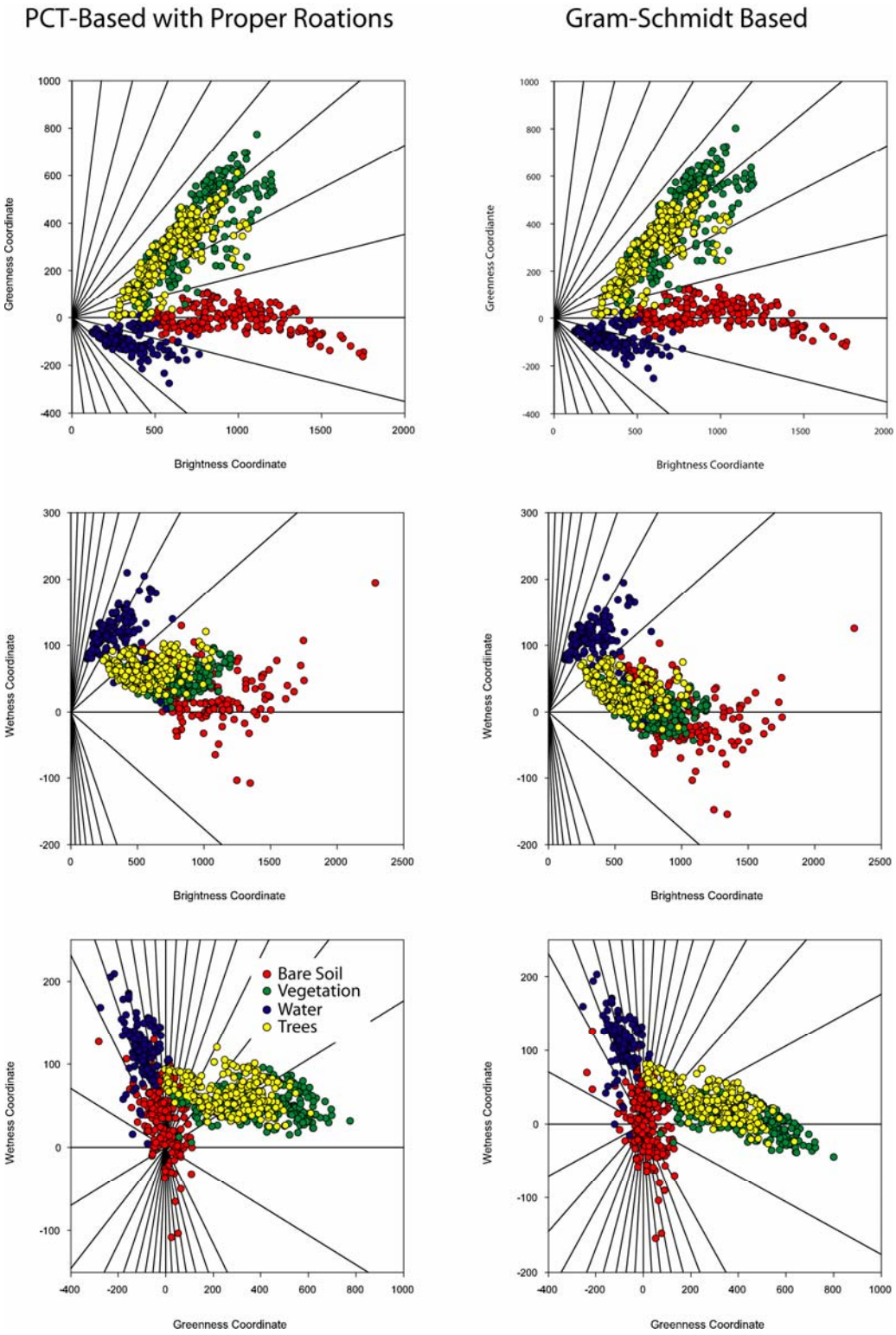

Figure 2. Comparison of Tasseled Cap space using derivations of PCT with rotation and Gram-Schmidt process. Only slight differences in the Brightness-Greenness plane while trends are more evident in higher order axes. Note the Wetness axes on the bottom row of plots have different scales. Guidelines are plotted at 10° increments.

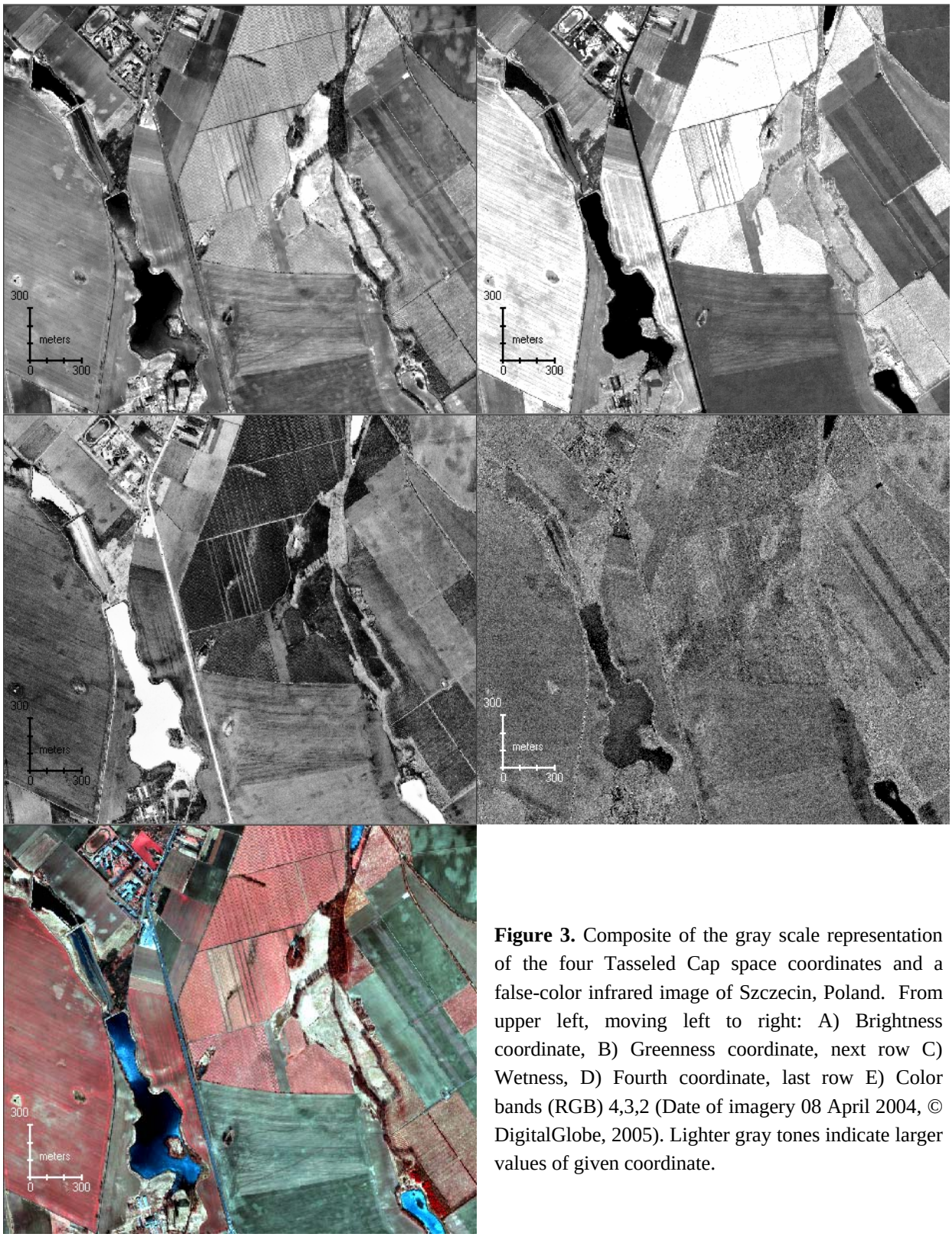

Figure 3. Composite of the gray scale representation of the four Tasseled Cap space coordinates and a false-color infrared image of Szczecin, Poland. From upper left, moving left to right: A) Brightness coordinate, B) Greenness coordinate, next row C) Wetness, D) Fourth coordinate, last row E) Color bands (RGB) 4,3,2 (Date of imagery 08 April 2004, © DigitalGlobe, 2005). Lighter gray tones indicate larger values of given coordinate.

In every image, regardless of which of the three methods were used, the total percent of variance explained by the first three coordinates of Tasseled Cap space were between 99.72 and 99.98%. Furthermore, given only the first two coordinate axes, 98.33% of the variance or greater was explained. Again, this result is analogous to a 2-D ellipse fixed within a 4-D space. The total variance found in the direction of the $\mathbf{u}_{Wetness}$ axis was negligible and exacerbates the issue of limited contrast required to distinguish water and low reflectance invariant features.

Of the three-derivation techniques, the Gram-Schmidt-based method was chosen to represent the correct $\mathbf{W}_{TC}$ for the TCT of QB 11-bit DRA-off data. Again, these are reported as column vectors in Equation 7. The selection was based on the final shape of the data when plotted in Tasseled Cap space. In Figure 2, the Greenness-Wetness plane shows a negative trend of the vegetation data in the opposite direction of Wetness and the data remained tightly grouped in the Gram-Schmidt derivation. One can argue that the PCT-based derivation could be rotated to match the Gram-Schmidt directions; however, this process would be highly bias and one would nonetheless require the Gram-Schmidt derivation for comparison.

ACKNOWLEDGMENTS

We would like to thank the DigitialGlobe, Inc. for access to their imagery archive. Thank you to Brett Thomassie, Jeff Liedtke and Alex Diamond, all of DigitalGlobe, Inc. We acknowledge the support of The University of Mississippi Geoinformatics Center and the Enterprise for Innovative Geospatial Solutions. Finally, we appreciate the open source software developed by Foxes Team of Italy, which provided instrumental in the derivation of the coefficients.

REFERENCES

Crist, E.P. and R.C. Cicone (1984). A Physically-Based Transformation of Thematic Mapper Data -- The TM Tasseled Cap. *IEEE Transactions on Geoscience and Remote Sensing*, 22(3): 256-263.

Crist, E.P. and R.J. Kauth (1986). The Tasseled Cap De-Mystified. *Photogrammetric Engineering and Remote Sensing*, 52(1):81-86.

Horne, J.H. (2003). A Tasseled Cap Transform for IKONOS Images. In: *ASPRS Annual Conference Proceedings*, Anchorage, Alaska.

Huang, C., B. Wylie, L. Yang, C. Homer, and G. Zylstra (2002). Derivation of a tasselled cap transformation based on Landsat 7 at-satellite reflectance. *International Journal of Remote Sensing*. 23:1741-1748.

Kauth, R.J. and G.S. Thomas (1976). The Tasseled Cap – a graphical description of the spectral-temporal development of agricultural crops as seen by Landsat. In: *Proceedings of the Symposium on Machine Processing of Remotely Sensed Data*. Purdue University, West Lafayette, Indiana, pp. 4B41-4B51.

Team Foxes (2004). Matrices and Linear Algebra. 5th Ed.

Yarbrough, L.D., G. Easson, and J.S. Kuszmaul (2005). Using At-Sensor Radiance and Reflectance Tasseled Cap Transforms Applied to Change Detection for the ASTER Sensor, Eds. R. L.King and N. H. Younan, In: *Proceedings of the Third International Workshop on the Analysis of Multi-Temporal Remote Sensing Images*, 16-18 May 2005, Beau Rivage Resort and Casino, Biloxi, Mississippi, USA.

Zhang, X., C.B. Schaaf, M.A. Friedl, A.H. Strahler, F. Gao, and J.C.F.H. Hodges (2002). MODIS Tasseled Cap Transformation and Its Utility. In: *Proceedings of the International Geoscience and Remote Sensing Symposium* (IGARSS'02), Toronto, Canada, pp. 24-28.